Evolution of the bosonic spectral density of the high-temperature superconductor $Bi_2Sr_2CaCu_2O_{8+\delta}$

J. Hwang,[1,*] T. Timusk,[1,2] E. Schachinger,[3] and J. P. Carbotte[1,2]
[1]*Department of Physics and Astronomy, McMaster University, Hamilton, Ontario L8S 4M1, Canada*
[2]*The Canadian Institute of Advanced Research, Toronto, Ontario M5G 1Z8, Canada*
[3]*Institute of Theoretical and Computational Physics, Graz University of Technology, A-8010 Graz, Austria*
(Received 26 March 2007; published 20 April 2007)

We demonstrate that an Eliashberg inversion of the optical self-energy, based on maximum-entropy considerations, can be used to extract in numerical form the bosonic excitation spectra of high-transition-temperature superconductors. In $Bi_2Sr_2CaCu_2O_{8+\delta}$ we explicitly show that the bosonic mode that dominates the self-energy at low temperatures and small energies directly evolves out of a balanced transfer of spectral weight to the mode from the continuum just above it. This redistribution starts already at 200 K in optimally doped materials but is much weaker in overdoped samples. This finding presents a challenge to theories of the spin susceptibility and to neutron scattering experiments in high-temperature superconductors.

DOI: 10.1103/PhysRevB.75.144508 PACS number(s): 74.25.Gz, 74.62.Dh, 74.72.Hs

I. INTRODUCTION

The phenomenon of high-temperature superconductivity, discovered in copper oxides 20 years ago,[1] continues to challenge both theorists and experimentalists. From the beginning it was clear that magnetism was an important part of the solution to this puzzle. In conventional superconductors the spectrum of pairing excitations was successfully extracted as an electron-phonon spectral function $\alpha^2F(\Omega)$ using an inversion of experimental tunneling[2] and optical data[3] based on the Eliashberg equations. In principle this spectrum contains information on the microscopic interactions among electrons mediated by boson exchanges which are needed to describe superconductivity and can be calculated from band structure information.[4] The primary tools used to map out the magnetic excitations in high-temperature superconductors have been neutron scattering and nuclear magnetic resonance. The picture that has emerged from these studies is a not-well-understood spectrum of excitations dominated by a continuous background extending to unusually high energies, sometimes called the Millis-Monien-Pines (MMP) spectrum[5–9] which evolves into a broad peak in the local ($\mathbf{q}$-integrated) susceptibility at low temperatures along with a sharp resonance in the superconducting state centered at $\mathbf{q}=(\pi,\pi)$, the 41-meV mode, named after its frequency in optimally doped $YBa_2Cu_3O_{6+\delta}$ (Y-123).[10–15] This sharp resonance has also been seen in $Tl_2Ba_2CuO_{6+\delta}$ (Ref. 16) and in $Bi_2Sr_2CaCu_2O_{8+\delta}$ (Bi-2212).[17,18] The magnetic resonance mode,[6,19–22] phonons,[23–25] and broad continuum[7,26–28] in the bosonic spectra have been proposed as candidates for the pairing glue in the copper oxides. Here we use a broader definition of the magnetic resonance as the peak that develops in the local magnetic susceptibility at low temperatures. Some theories of the spin susceptibility have predicted that the magnetic resonance develops out of the MMP continuum[6,29] when the superconducting gap forms. However, so far no consensus has been achieved. To throw light on this issue we have undertaken a study of the spectrum of excitations responsible for the self-energy of the charge carriers as a function of temperature and doping in three Bi-2212 systems using optical spectroscopy focusing on the overdoped region of the phase diagram. We clearly observe experimentally the evolution of a strong peak in the integrated bosonic response developing from the broad continuum just above it as a function of both *temperature* and *doping*.

We present our theoretical approach in Sec. II and our results for the electron-boson spectral functions across the doping and temperature range studied here in Sec. III. Section IV elaborates on the analysis of the spectra obtained, and Sec. V includes a discussion and conclusions.

II. THEORETICAL APPROACH

The optical self-energy $\Sigma^{op}(\omega)$, which involves a momentum average, is closely related to the quasiparticle self-energy measured by angle-resolved photoemission spectroscopy which is momentum specific. The optical self-energy is defined in terms of an extended Drude formula[26]

$$\sigma(\omega) \equiv \frac{i}{4\pi}\frac{\omega_p^2}{\omega - 2\Sigma^{op}(\omega)}, \tag{1}$$

where ω_p is the plasma frequency and $\Sigma^{op}(\omega)\equiv\Sigma_1^{op}(\omega)+i\Sigma_2^{op}(\omega)$. The optical scattering rate is defined by $1/\tau^{op}(\omega)\equiv -2\Sigma_2^{op}(\omega)$. The optical conductivity $\sigma(\omega)$ can be found through a Kramers-Kronig transformation of the reflectance which is measured directly. The numerical inversion of the optical scattering rate is based on an Eliashberg formalism. We start with a deconvolution of the approximate relation[30,31]

$$\frac{1}{\tau^{op}(\omega;T)} = \int_0^\infty d\Omega K(\omega,\Omega;T) I^2\chi(\Omega), \tag{2}$$

where T is temperature, $K(\omega,\Omega;T)$ is a kernel determined from theory, and $I^2\chi(\Omega)$ is the bosonic spectrum. For the deconvolution we utilized the maximum-entropy method (MaxEnt), originated by Jaynes.[32] For the kernel we use

$$K(\omega,\Omega;T) = \frac{\pi}{\omega}\{2\omega\coth(\Omega/2T) - (\omega+\Omega) \times \coth[(\omega+\Omega)/2T] + (\omega-\Omega)\coth[(\omega-\Omega)/2T]\} \quad (3)$$

for the normal state[33] and

$$K(\omega,\Omega;T=0) = \frac{2\pi}{\omega}\langle(\omega-\Omega)\theta(\omega-2\Delta_0(\vartheta)-\Omega) \times E(\sqrt{1-4\Delta_0^2(\vartheta)/(\omega-\Omega)^2})\rangle_\vartheta \quad (4)$$

for the superconducting state[34] at zero temperature where $\langle\cdots\rangle_\vartheta$ denotes the angular average over $[0,\pi/4]$ and $E(x)$ is a complete elliptic integral of second kind. Here $\Delta_0(\vartheta) = \Delta_0\cos(2\vartheta)$ reflects the d-wave symmetry of the superconducting order parameter. For the superconducting state at finite temperature we adjust the size of the maximum gap, Δ_0, according to a BCS temperature variation. This provides us with a first model for $I^2\chi(\Omega)$ of Eq. (2) which we further refine by using this model in the full Eliashberg equations. The needed adjustments are made (never large for normal-state data, more involved in the superconducting state) through a least-squares fit of the resulting optical scattering rate to the experimental data. Such a procedure helps to eliminate at least some of the ambiguities inherent to the MaxEnt deconvolution of Eq. (2). The result is our final model for the electron-exchange boson spectral density. Maximum entropy, however, provides us with the most probable spectrum within the framework of whatever external constraints are imposed on the size, shape, and extent in frequency of the spectral function $I^2\chi(\Omega)$. An obvious constraint is that it be positive. The spectrum obtained by such a procedure, however, does contain elements necessary to compensate any shortcomings the Eliashberg theory might have in its application to the cuprates.

As we use classical MaxEnt[30] only, we have a second constraint, the default model which dominates the highest-frequency part of the inverted spectra. It was set to a constant 0.1 (in one case, $T=27$ K, sample OPT96A, the value 0.05 was used) over the whole energy range, and we see that all but one of the spectra shown in Figs. 2(a)–2(c) level smoothly at this value which is below all the important structures in the energy region $0 \leq \hbar\omega \leq 400$ meV. Thus, the default model we chose does not obscure possibly important parts of the inverted spectra. Another parameter which enters the MaxEnt inversion is σ which measures the amount of uncorrelated Gaussian noise attached to the data.[30] This parameter ranged between 2.5 and 7 with the larger values used for superconducting-state data to compensate for the fact that Eq. (4) is a rather poor model for finite-temperature data. Small values of σ force MaxEnt to follow closely the experimental $1/\tau^{op}(\omega)$ data which only works well if the model used for the kernel $K(\omega,\Omega;T)$ is a rather good one, as is the case for the normal-state kernel, Eq. (3).

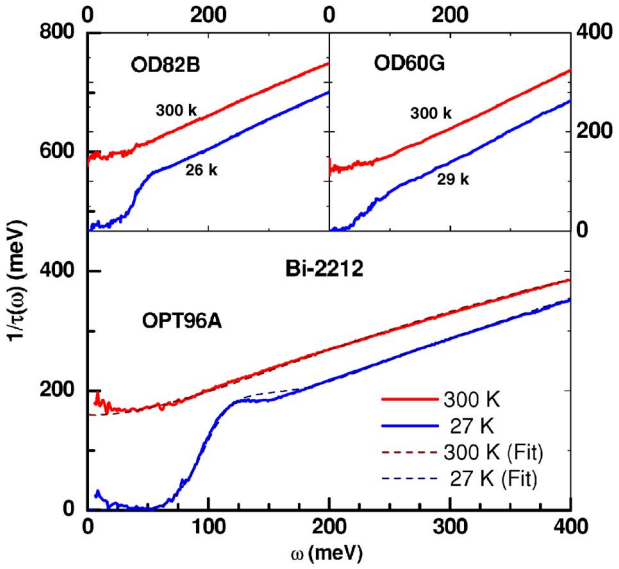

FIG. 1. (Color online) Lower panel: the optical scattering rate $1/\tau^{op}(\omega)$ as a function of ω of $Bi_2Sr_2CaCu_2O_{8+\delta}$ at three doping levels. Solid lines are data and dashed lines are a fit using the Eliashberg formalism. We attribute the upturn in scattering below 50 meV to localization effects. The two top panels show the optical scattering rates of our two overdoped samples. They show no low-frequency localization effects.

III. RESULTS FOR THE ELECTRON-BOSON SPECTRAL DENSITY

We take the imaginary part of the optical self-energy of Bi-2212 from a previous study[26] of an optimally doped and two overdoped samples. We note that the optimally doped sample is yttrium doped and, thus, somewhat different from conventional optimally doped Bi-2212, having a more ordered structure and a higher T_c.[35] Underdoped systems show pseudogap behavior not yet incorporated in the inversion formalism and are not treated here. In Fig. 1 we show our fit (dashed lines) to data (solid lines) as an example for our optimally doped sample OPT96A at two temperatures: dark lines are for $T=300$ K (normal) and light lines for $T=27$ K (superconducting). The fits are very good except for two small spectral regions near zero energy for both states and near the overshoot region ($\sim$120 meV) in the superconducting state. Above 125 meV, in the superconducting state, the theoretical curve has a slight slope while the experimental data are flat. The discrepancy near zero energy may come from impurity localization which is observed in some cuprate systems and which in the overshoot region stems from our attempt to produce the overall best possible fit to the data. We note that the optimally doped sample shows the strongest localization but this does not affect the main sharp peak in $I^2\chi(\Omega)$. The two overdoped samples OD82B ($T_c=82$ K) and OD60G ($T_c=60$ K) show negligible localization (see the insets in Fig. 1).

In Figs. 2(a)–2(c) we plot the extracted bosonic spectral densities $I^2\chi(\omega)$ of Bi-2212. We note that they extend in frequency up to at least 400 meV which is consistent with a spin fluctuation or other electronic mechanisms. We also ob-

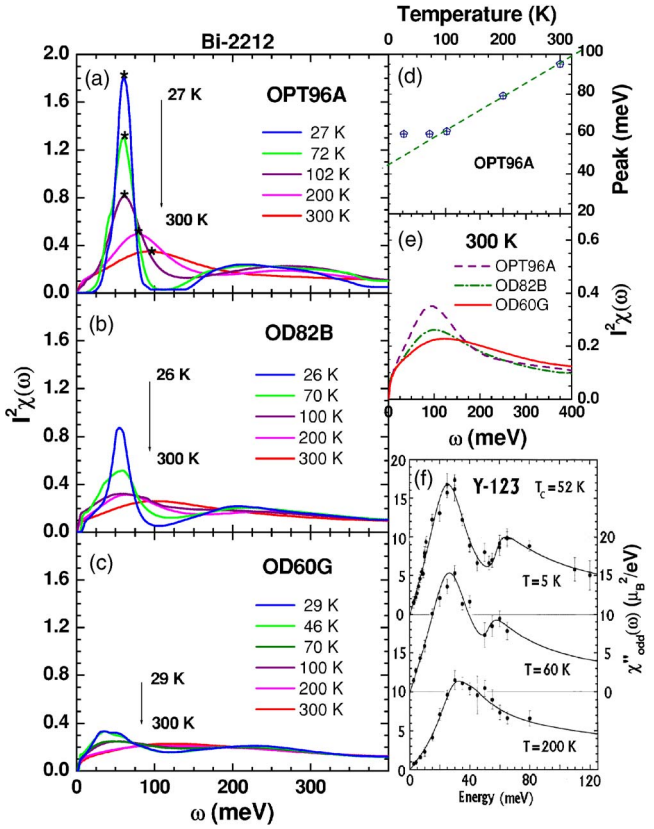

FIG. 2. (Color online) The bosonic spectral density $I^2\chi(\omega)$ of $Bi_2Sr_2CaCu_2O_{8+\delta}$ (a)–(c). The doping- and temperature-dependent bosonic function for three doping levels [T_c=96 K (OPT96A), 82 K (OD82B), and 60 K (OD60G)]. At room temperature all samples exhibit a broad continuum background shown in panel (e). On lowering the temperature the broad background peak in the 300-K spectrum evolves into a somewhat sharper low-energy peak with a deep valley above it. The spectral weight gained in the peak is roughly balanced by the spectral weight loss in the valley in all three samples. With increasing doping the intensity of the peak and intensity lost in the valley are significantly weakened [see Fig. 4(b)]. Panel (d) shows the temperature dependence of the frequency of the peak maximum in OPT96A marked by a star. Panel (f) shows the local magnetic susceptibility of underdoped Y-123 from neutron scattering (Refs. 5, 8, and 36). While this is a different copper oxide system from the ones given in panels (a), (b), and (c) we note a qualitatively similar temperature evolution of panel (a).

serve dramatic temperature and doping dependences. The room-temperature spectra show a broad continuum which exhibits some doping dependence as shown in panel 2(e). At lower doping levels, the broad peak in the spectrum becomes somewhat stronger and shifts to lower frequencies. The temperature and doping dependence, as we move from panel 2(a) to panel 2(c), is more striking. As the temperature is lowered nearly all the spectral weight below 130 meV in the optimally doped material is moved to a resonance peak while in the overdoped region less and less of the continuum spectral weight is transferred to this peak. A similar temperature dependence has been observed in the local spin susceptibility by magnetic neutron scattering experiments[8] in underdoped $YBa_2Cu_3O_{6.6}$ [see Fig. 2(f)]. The broad peak in the room-temperature spectrum, at 97 meV in panel 2(a), shifts continuously to lower energies as its intensity grows as the temperature is lowered. Panel 2(d) shows that the peak position is approximately linear in temperature above T=100 K and saturates to 60 meV below this temperature. What is notable about this process is that this evolution takes place through a transfer of spectral weight from frequencies above the peak, leaving a valley between 100 to 150 meV. In addition, there is a well-developed 22 meV cutoff on the low-frequency side of the peak in the superconducting state. Such a cutoff in the bosonic spectral density is consistent with the observations of spin-polarized neutron scattering for optimally doped Y-123 with T_c=91 K.[36] As shown in Figs. 2(b) and 2(c) for higher doping levels this low-frequency cutoff in the bosonic spectral density becomes small and, while the resonance mode can still be discerned, it weakens significantly.[26] In our most overdoped sample (OD60G) only a small fraction of spectral weight in the bosonic spectrum contributes to the temperature redistribution. The optical resonance is effectively gone in this case. The behavior of this heavily overdoped sample is very similar to what was found[37,38] for a heavily overdoped thallium compound in which no optical resonance was observed. In that case, the optical data were fit, instead, with the use of a simple MMP spectrum.[38]

It is interesting to note that Tu *et al.*[39] also observe in their optimally doped Bi-2212 sample that the optical resonance at 43 meV extends into the normal state and can clearly be seen at 100 K from inversion. The MaxEnt analysis by Schachinger *et al.*[30] confirmed this result and, moreover, demonstrated that the resonance existed even at 200 K but now shifted to about 60 meV. This is qualitatively quite consistent with what we report here. In the light of the data presented by Tu *et al.*[39] and now here, it would be important to have independent confirmation of the phenomenon of the existence of an optical resonance in the normal state of optimally doped Bi-2212 samples up to quite high temperatures (~200 K) from other probes such as magnetic neutron scattering.

There are no neutron scattering data on the local spin susceptibility of Bi-2212 over a wide range of temperatures and doping levels. In their absence, the best we can do is to show in Fig. 2(f) the local (**q**-integrated) magnetic susceptibility $\chi''_{odd}(\omega)$ from a neutron scattering study of underdoped Y-123 (Refs. 5 and 8) to compare its temperature-dependent spectral weight redistribution with $I^2\chi(\omega)$ of our optimally doped Bi-2212 (OPT96A) sample. Although they are different copper oxide systems and at different doping levels, they qualitatively contain some of the temperature-dependent features which we find in our inverted optical spectra. A similar spectral redistribution of the local magnetic susceptibility has been observed by Dai *et al.*[14] However, it was not widely recognized or confirmed by other experiments. Here we find that the spectral redistribution occurs mainly in the low-frequency region below 200 meV and is strongly doping dependent on the overdoped side of the phase diagram. Very recently the spin susceptibility of LSCO (Ref. 40) was also found to involve two energy scales, although very different from the ones observed here. Nevertheless, this indicates that composite spin susceptibility spectra may be a common occurrence in the cuprates.

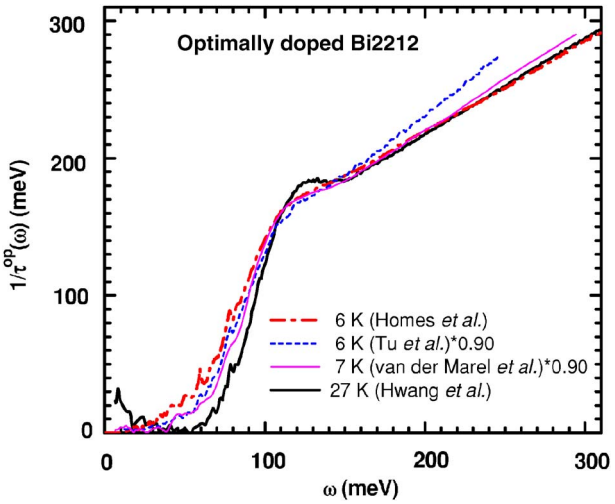

FIG. 3. (Color online) The optical scattering rate for four different samples of optimally doped Bi2212. Dash-dotted line (red) from Homes (Ref. 41) dashed line (blue) from Tu *et al.*(Ref. 39), light solid line (purple) from van der (Ref. *et al.*[42]), and heavy solid line (black) from Hwang *et al.*(Ref. 26).

Alternatively, we can look at the spectrum at low temperatures in Fig. 2(a) as the development of a large ~130-meV gap in the spin fluctuation spectrum which closes with increasing temperature with a mode in the middle of the gap at 60 meV. Such a transformation has been considered by Abanov and Chubukov[6] but with the gap arising at $2\Delta_0$ with Δ_0 the superconducting gap. Here we find a much larger gap that starts to form already at $T=200$ K, well above T_c. A model $I^2\chi(\Omega)$ with a complete gap rather than a valley at low temperatures in the superconducting state, decreasing in size with increasing temperature, would fit equally well the optical data for the superconducting state on which our analysis is based.

We note, furthermore, that the optical resonance peak in Fig. 2(a) is at 60 meV and this energy is considerable larger than found by Tu *et al.*[39] for another sample of optimally doped Bi2212 where it is at 43 meV as in the neutron study.[18] Our sample is Y doped and has a higher $T_c=96$ K than does the sample of Tu *et al.* ($T_c=91$ K). This could account in part for the difference in resonance energy. We have examined similar Y-doped Bi2212 samples used by van der Marel *et al.*[42] and estimated a resonance energy of ~54 meV instead of 60 meV, indicating that doping with Y does indeed increase the resonance energy. It would be important to verify this by neutron scattering. More details are found in Fig. 3 where we compare results for the optical scattering rate $1/\tau^{op}(\omega)$ in optimally doped Bi2212 obtained on various samples by different groups. The (red, dash-dotted line) data are those of Homes *et al.*[41] The main rise in $1/\tau^{op}(\omega)$, associated with the position of the resonance mode displaced by the superconducting gap, is lowest in this sample. Next comes the sample of Tu *et al.*[39] (blue, dashed line), then that of van der Marel *et al.*[42] (purple, light solid line), and finally ours (Hwang *et al.*[26]) (black, heavy solid line). There is clearly some variation from sample to sample and from group to group, reflecting differences in Ω_{peak} and superconducting gap values. Our sample shows a rather high value of Ω_{peak}. A similar situation holds for our overdoped sample with a T_c of 82 K where the optical resonance is at 55 meV, again quite high. In this case, however, the MaxEnt fit which was designed to give the best overall fit did not accurately give the position of the main rise in the optical scattering rate. If we had concentrated in our fit on the best possible reproduction of the main rise, we would have obtained ~47 meV. These details, however, are not critical to this study which deals with overall spectral weight distributions as a function of temperature and doping.

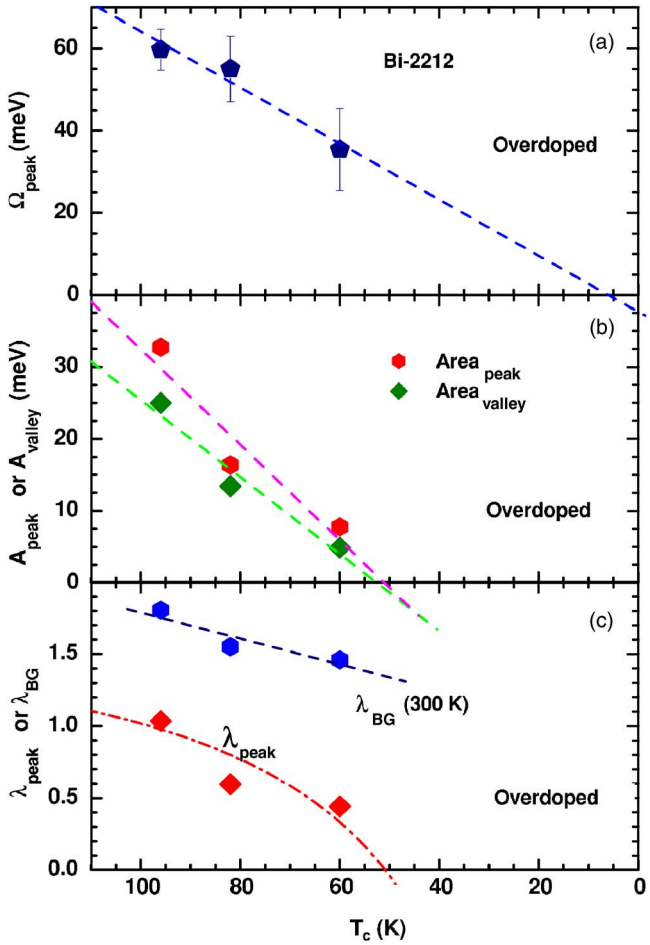

FIG. 4. (Color online) T_c-dependent properties of the peak and the valley (see text). (a) The central peak frequency is proportional to T_c, i.e., $\Omega_{peak}=8.0k_BT_c$, and the dashed line is a linear fit. (b) The peak and valley are closely connected, have a very similar T_c dependence, and vanish at the same $T_c\approx 50$ K. The dashed lines are a linear fit. (c) The coupling constant λ_{peak} vanishes at the same T_c as the peak and valley. The dash-dotted line is obtained by using the linearly fitted center frequency [dashed line (a)] and the area under the peak [(b)], i.e., $\lambda_{peak}\simeq 2A_{peak}/\Omega_{peak}$.

IV. ANALYSIS OF SPECTRA

To study quantitatively the changes in the bosonic spectra we subtract the room-temperature spectrum from the lower-temperature spectra. We clearly observe a peak and a valley in the difference spectra. In Fig. 4 we display the T_c depen-

TABLE I. Superconducting (SC) gap values of our three samples obtained from our analysis.

Samples	OPT96A		OD82B		OD60G	
Temperature T (K)	27	72	26	70	29	46
SC gap Δ (meV)	23	18	21	14	13	9.3

dence of various properties of the peak and valley in the bosonic spectra. Figure 4(a) shows the center frequency of the peak, Ω_{peak}, versus T_c at our lowest measured temperatures. We find $\Omega_{peak} \approx 8.0 k_B T_c$, which is similar to the temperature dependence of the magnetic resonance mode ($\Omega_{res} \approx 5.3 k_B T_c$). As discussed in detail above, our samples give a higher value of Ω_{peak} than those in Ref. 18 and there are additional uncertainties associated with the inversion process including gap values. Here we take the gap from numerical solutions of the Eliashberg equations written for the superconducting state assuming the gap to have d-wave symmetry.[34] Our results for the amplitude (Δ) of the gap are presented in Table I. These are somewhat lower than some quoted in the literature.[43] A higher value for Δ will bring down the frequency of Ω_{peak}. [The structures in the optical characteristics fall at energies Ω plus a fraction of twice the gap (exactly twice for s waves).] In Fig. 4(b) we plot the area under the peak and the area in the valley above it as a function of the critical temperature for our lowest temperature (we also include the low-frequency cutoff as part of the valley). The two areas estimated by subtracting the 300-K curve show the same trend; both decrease rapidly as T_c decreases in the overdoped region and their extrapolation shows that they vanish at the same T_c near 50 K. While the criterion used to determine the areas under the peak and valley is not unique, we find that the total spectral weight up to 400 meV is conserved to within 15% which may indicate a small frequency dependence of the coupling constant I^2 in $I^2\chi(\Omega)$. It is also necessary to emphasize that in MaxEnt and consequently also in our improved method (least-squares fit using Eliashberg equations), the area under the spectrum can change slightly. For instance, we produced fits for the optimally doped Bi-2212 sample (T_c=96 K) in which the valley between 90 and 140 meV at 27 K is replaced by a full gap with the quality of the fit not seriously affected. There is little change in the spectral weight redistribution, however.

We calculated the T_c-dependent coupling constant $\lambda(T_c) = 2\int_0^{\omega_c} I^2\chi(\Omega, T_c)/\Omega d\Omega$ using only the peak (λ_{peak}) or the continuum (λ_{BG}) for $I^2\chi(\Omega)$. For λ_{BG} the cutoff frequency ω_c was taken to be 400 meV and the 300-K $I^2\chi(\Omega)$ spectrum was used. For the peak we take only the part above the 300-K background. The results are shown in Fig. 4(c). The peak coupling constant λ_{peak} decreases rapidly, extrapolating to zero at T_c=50 K. The coupling constant of the background λ_{BG} shows a weaker dependence on T_c.

V. DISCUSSION AND CONCLUSIONS

Our analysis of the optical data has provided detailed information on the redistribution with temperature and doping levels of the spectral weight in the inelastic scattering spectral function. This analysis of optical data, based on an Eliashberg inversion, is the only existing method to date which can be used to study the evolution of the bosonic spectral density as a function of doping and temperature across the phase diagram of high-T_c oxides. Furthermore, this analysis can also be applied to other existing optical spectra to get insight into the excitation spectra that couple charge carriers. Our central finding is that the optical resonance peak which becomes prominent at low temperatures in our optimally doped sample forms mainly through the transfer of spectral weight from the energy region immediately above it. This constitutes strong evidence that the peak and background in the bosonic spectral function have the same microscopic origin. In non-yttrium-doped Bi-2212 samples the optical resonance in the superconducting state was identified by neutron scattering experiments as a spin-1 resonance at the same energy—namely, 43 meV. Thus, we predict that in yttrium-doped Bi-2212 samples the spin-1 resonance will be found at ~60 meV in the local spin susceptibility. Moreover, the room-temperature background spectrum [Fig. 2(e)] of all these samples resembles an MMP form[7] which extends to at least 400 meV. Thus, we conclude that this background which dominates the inelastic scattering above T_c is magnetic in origin. Finally, we confirm that the spin-1 resonance in the superconducting state shifts to lower energies with increasing oxygen doping level until, in the overdoped side, it disappears completely given high enough doping levels (in our case at a T_c of about 50 K).[26]

We also observe a temperature scale[30,39] around 200 K in optimally doped Bi-2212 where the magnetic spectrum begins to soften and develops an optical resonance peak in the $I^2\chi(\Omega)$ spectra. This scale shifts to lower temperatures with increasing oxygen doping level (~100 K in sample OD82B) until it cannot be observed any longer. (Sample OD60G does not show such a temperature scale.) To our knowledge the origin of this peak in the normal state has not yet been identified and current theories do not account for this phenomenon.

Finally, we note that the MaxEnt inversion and the Eliashberg analysis in the superconducting state involve a large amount of mathematics and one might legitimately question some of the approximations that were used to obtain $K(\omega, \Omega; T)$ and whether our inversion is unique. We would like to observe that, in hindsight, we can see already in the raw reflectance data all the important features of our final conclusions: the onset of strong scattering at the gap+mode frequency and the long tail extending up to 400 meV in the background that persists up to room temperature. Of course these features have been understood from the beginning of the field. What is different in our analysis is the transfer of spectral weight from just above the mode to the mode as the temperature is lowered. In the raw data this is the region of the low-temperature overshoot in the scattering rate. Previous methods of analysis simply gave a region of unphysical negative bosonic spectrum here. We now know that this region corresponds to a gap in the bosonic density of states that develops as spectral weight is transferred to the mode.

ACKNOWLEDGMENTS

This work has been supported by the Canadian Natural Science and Engineering Research Council and the Canadian Institute of Advanced Research. We acknowledge the contribution of Genda Gu and Hiroshi Eisaki in growing the crystals that we used. We have profited from discussions with Philip Anderson, Philip Bourges, Andrey Chubukov, Matthias Eschrig, Bernhard Keimer, and Chandra Varma.

*Electronic address: hwangjs@mcmaster.ca

[1] T. G. Bednorz and K. A. Müller, Z. Phys. B: Condens. Matter **64**, 189 (1986).
[2] J. P. Carbotte, Rev. Mod. Phys. **62**, 1027 (1990).
[3] B. Farnworth and T. Timusk, Phys. Rev. B **10**, 2799 (1974); **14**, 5119 (1976).
[4] P. G. Tomlinson and J. P. Carbotte, Phys. Rev. B **13**, 4738 (1976).
[5] P. Bourges, H. F. Fong, L. P. Regnault, J. Bossy, C. Vettier, D. L. Milius, I. A. Aksay, and B. Keimer, Phys. Rev. B **56**, R11439 (1997).
[6] Ar. Abanov and A. V. Chubukov, Phys. Rev. Lett. **83**, 1652 (1999).
[7] A. J. Millis, H. Monien, and D. Pines, Phys. Rev. B **42**, 167 (1990).
[8] H. F. Fong, P. Bourges, Y. Sidis, L. P. Regnault, J. Bossy, A. Ivanov, D. L. Milius, I. A. Aksay, and B. Keimer, Phys. Rev. B **61**, 14773 (2000).
[9] V. Hinkov, P. Bourges, S. Pailhes, Y. Sidis, A. Ivanov, C. T. Lin, D. P. Chen, and B. Keimer, arXiv:cond-mat/0601048 (unpublished).
[10] J. Rossat-Mignod, L. P. Regnault, C. Vettier, P. Bourges, P. Burlet, J. Bossy, J. Y. Henry, and G. Lapertout, Physica C **185-189**, 86 (1991).
[11] H. A. Mook, M. Yethiraj, G. Aeppli, T. E. Mason, and T. Armstrong, Phys. Rev. Lett. **70**, 3490 (1993).
[12] H. F. Fong, B. Keimer, P. W. Anderson, D. Reznik, F. Dogan, and I. A. Aksay, Phys. Rev. Lett. **75**, 316 (1995).
[13] H. A. Mook, P. Dai, S. M. Hayden, G. Aeppli, T. G. Perring, and F. Dogan, Nature (London) **395**, 580 (1998).
[14] P. Dai, H. A. Mook, S. M. Hayden, G. Aeppli, T. G. Perring, R. D. Hunt, and F. Dogan, Science **284**, 1344 (1999).
[15] M. Eschrig, Adv. Phys. **55**, 47 (2006).
[16] H. He, P. Bourges, Y. Sidis, C. Ulrich, L. P. Regnault, S. Pailhès, N. S. Berzigiarova, N. N. Kolesnikov, and B. Keimer, Science **295**, 1045 (2002).
[17] H. F. Fong, P. Bourges, Y. Sidis, L. P. Regnault, A. Ivanov, G. D. Gu, N. Koshizuka, and B. Keimer, Nature (London) **398**, 588 (1999).
[18] H. He, Y. Sidis, P. Bourges, G. D. Gu, A. Ivanov, N. Koshizuka, B. Liang, C. T. Lin, L. P. Regnault, E. Schoenherr, and B. Keimer, Phys. Rev. Lett. **86**, 1610 (2001).
[19] M. R. Norman and H. Ding, Phys. Rev. B **57**, R11089 (1998).
[20] J. C. Campuzano, H. Ding, M. R. Norman, H. M. Fretwell, M. Randeria, A. Kaminski, J. Mesot, T. Takeuchi, T. Sato, T. Yokoya, T. Takahashi, T. Mochiku, K. Kadowaki, P. Guptasarma, D. G. Hinks, Z. Konstantinovic, Z. Z. Li, and H. Raffy, Phys. Rev. Lett. **83**, 3709 (1999).
[21] J. F. Zasadzinski, L. Ozyuzer, L. Coffey, K. E. Gray, D. G. Hinks, and C. Kendziora, Phys. Rev. Lett. **96**, 017004 (2006).
[22] K. Terashima, H. Matsui, D. Hashimoto, T. Sato, T. Takahashi, H. Ding, T. Yamamoto, and K. Kadowaki, Nat. Phys. **2**, 27 (2006).
[23] A. Lanzara, P. V. Bogdanov, X. J. Zhou, S. A. Kellar, D. L. Feng, E. D. Lu, T. Yoshida, H. Eisaki, A. Fujimori, K. Kishio, J.-I. Shimoyama, T. Noda, S. Uchida, Z. Hussain, and Z.-X. Shen, Nature (London) **412**, 510 (2001).
[24] G.-H. Gweon, T. Sasagawa, S. Y. Zhou, J. Graf, H. Takagi, D.-H. Lee, and A. Lanzara, Nature (London) **430**, 187 (2004).
[25] X. J. Zhou, Junren Shi, T. Yoshida, T. Cuk, W. L. Yang, V. Brouet, J. Nakamura, N. Mannella, Seiki Komiya, Yoichi Ando, F. Zhou, W. X. Ti, J. W. Xiong, Z. X. Zhao, T. Sasagawa, T. Kakeshita, H. Eisaki, S. Uchida, A. Fujimori, Zhenyu Zhang, E. W. Plummer, R. B. Laughlin, Z. Hussain, and Z.-X. Shen, Phys. Rev. Lett. **95**, 117001 (2005).
[26] J. Hwang, T. Timusk, and D. G. Gu, Nature (London) **427**, 714 (2004).
[27] J. P. Carbotte, E. Schachinger, and D. N. Basov, Nature (London) **401**, 354 (1999).
[28] E. Schachinger and J. P. Carbotte, Phys. Rev. B **62**, 9054 (2000).
[29] See, for example, D. K. Morr and D. Pines, Phys. Rev. Lett. **81**, 1086 (1998) and references therein.
[30] E. Schachinger, D. Neuber, and J. P. Carbotte, Phys. Rev. B **73**, 184507 (2006).
[31] S. V. Dordevic, C. C. Homes, J. J. Tu, T. Valla, M. Strongin, P. D. Johnson, G. D. Gu, and D. N. Basov, Phys. Rev. B **71**, 104529 (2005).
[32] E. T. Jaynes, Phys. Rev. **106**, 620 (1957).
[33] S. V. Shulga, O. V. Dolgov, and E. G. Maksimov, Physica C **178**, 266 (1991).
[34] J. P. Carbotte and E. Schachinger, Ann. Phys. **15**, 585 (2006).
[35] H. Eisaki, H. Kaneko, D. L. Feng, A. Damascelli, P. K. Mang, K. M. Shen, Z.-X Shen, and M. Greven, Phys. Rev. B **69**, 064512 (2004).
[36] P. Bourges, Y. Sidis, H. F. Fong, B. Keimer, L. P. Regnault, J. Bossy, A. S. Ivanov, D. L. Milius, and I. A. Aksay, in *High Temperature Superconductivity*, edited by S. E. Barnes, J. Ashkenazi, J. L. Cohn, and F. Zuo, AIP Conf. Proc. No. 483 (AIP, Woodbury, NY, 1999), p. 207.
[37] E. Schachinger and J. P. Carbotte, Phys. Rev. B **62**, 9054 (2000).
[38] Y. C. Ma and N. L. Wang, Phys. Rev. B **73**, 144503 (2006).
[39] J. J. Tu, C. C. Homes, G. D. Gu, D. N. Basov, and M. Strongin, Phys. Rev. B **66**, 144514 (2002).
[40] B. Vignolle, S. M. Hayden, D. F. McMorrow, H. M. Rønnow, B. Lake, C. D. Frost, and T. G. Perring, Nat. Phys. **3**, 163 (2007).
[41] C. C. Homes (private communication).
[42] D. van der Marel, H. J. A. Molegraaf, J. Zaanen, Z. Nussinov, F. Carbone, A. Damascelli, H. Eisaki, M. Greven, P. H. Kes, and M. Li, Nature (London) **425**, 271 (2003).
[43] T. Nakano, N. Momono, M. Oda, and M. Ido, J. Phys. Soc. Jpn. **67**, 2622 (1998).